The Astronomical Journal, 163:51 (7pp), 2022 February https://doi.org/10.3847/1538-3881/ac3cbe

KK 242, A Faint Companion to the Isolated Scd Galaxy NGC 6503

Igor D. Karachentsev[1], John M. Cannon[2], Jackson Fuson[2], John L. Inoue[2], R. Brent Tully[3], Gagandeep S. Anand[4], and Serafim S. Kaisin[1]
[1] Special Astrophysical Observatory, the Russian Academy of Sciences, Nizhnij Arkhyz, Karachai-Cherkessian Republic 369167, Russia; ikar@sao.ru
[2] Department of Physics & Astronomy, Macalester College, 1600 Grand Avenue, Saint Paul, MN 55105, USA
[3] Institute for Astronomy, University of Hawaii, 2680 Woodlawn Drive, Honolulu, HI 96822, USA
[4] Space Telescope Science Institute, 3700 San Martin Drive, Baltimore, MD 21218, USA
Received 2021 October 26; revised 2021 November 22; accepted 2021 November 22; published 2022 January 10

Abstract

Using Hubble Space Telescope imaging of the resolved stellar population of KK 242 = NGC 6503-d1 = PGC 4689184, we measure the distance to the galaxy to be 6.46 ± 0.32 Mpc and find that KK 242 is a satellite of the low-mass spiral galaxy NGC 6503 located on the edge of the Local Void. Observations with the Karl G. Jansky Very Large Array show signs of a very faint H I signal at the position of KK 242 within a velocity range of $V_{\rm hel} = -80 \pm 10$ km s^{-1}. This velocity range is severely contaminated by H I emission from the Milky Way and from NGC 6503. The dwarf galaxy is classified as the transition type, dIrr/dSph, with a total H I mass of $< 10^6 M_\odot$ and a star formation rate SFR(Hα) = −4.82 dex ($M_\odot$ yr^{-1}). Being at a projected separation of 31 kpc with a radial velocity difference of—105 km s^{-1} relative to NGC 6503, KK 242 gives an estimate of the halo mass of the spiral galaxy to be $\log(M/M_\odot) = 11.6$. Besides NGC 6503, there are eight more detached low-luminosity spiral galaxies in the Local Volume: M33, NGC 2403, NGC 7793, NGC 1313, NGC 4236, NGC 5068, NGC 4656, and NGC 7640, from whose small satellites we have estimated the average total mass of the host galaxies and their average total mass-to-K-band-luminosity $\langle M_T/M_\odot \rangle = (3.46 \pm 0.84) \times 10^{11}$ and $(58 \pm 19) M_\odot/L_\odot$, respectively.

Unified Astronomy Thesaurus concepts: Dwarf galaxies (416); Galaxies (573); Galaxy distances (590)

1. Introduction

The ratio of the stellar mass of a galaxy, M_*, to its halo mass, M_h, is a function of the integral luminosity and morphological type of the galaxy. The minimum M_h/M_* value is characteristic of spiral galaxies like the Milky Way and M31, and the value M_h/M_* is increasing toward objects of both high and low luminosity (Kourkchi & Tully 2017). The presence of such a minimum is usually explained by the high efficiency of star formation exactly in galaxies such as Milky Way and M31 (Correa & Schaye 2020). The M_h/M_* ratio for early-type galaxies (E, S0) is 2–3 times higher than that for spirals of the same stellar mass (Karachentseva et al. 2011; Bilicki et al. 2021; Posti & Fall 2021). This is probably due to the fact that in the last 10 Gyr, star formation in E, S0 galaxies took place at a very low rate.

Unlike massive spiral galaxies, the characteristic M_h/M_* value for low-luminosity spiral galaxies has not yet been reliably determined. According to Lapi et al. (2018), the disk-like galaxies with luminosities an order of magnitude lower than the Milky Way luminosity and rotation amplitudes $V_{\rm rot} < 120$ km s^{-1} have mainly increasing rotation curves. Extrapolation of the value $V_{\rm rot}$, measured within the optical radius of the galaxy (∼20 kpc), to a distance equal to the virial radius of the halo (∼120 kpc) introduces a significant uncertainty in the estimate of M_h.

The halo mass of a galaxy can be determined from the relative radial velocities and projected separations of its satellites. However, the number of satellites around low-mass galaxies is small. On average, there are only 1–2 dwarf satellites per one late-type spiral galaxy (Sc–Sd) with a luminosity in the K-band of $L_K/L_\odot \simeq (9.5\text{–}10.0)$ dex. For example, the M33 galaxy has two probable satellites: And XXII (Martin et al. 2009; Tollerud et al. 2012) and Tri III (Martinez Delgado et al. 2022). Carlin et al. (2016) undertook a search for faint satellites around another nearby isolated spiral galaxy of moderate luminosity, NGC 2403. To its collection of known satellites (DDO 44 and NGC 2366) they added one new object, MADCASHJ0742+65, the radial velocity of which has not yet been measured. Carlsten et al. (2020) has performed deep searches for new companions around 10 nearby massive galaxies. However, this study was limited to virial neighborhoods of galaxies with luminosities comparable to those of Milky Way and M31. Moderate luminosity galaxies were not considered.

Karachentseva & Karachentsev (1998) used the photografic Palomar sky survey POSS-II to search for nearby dwarf galaxies over the whole sky. Near the Scd galaxy NGC 6503 at a separation of 17′, they found an object of low surface brightness, called KK 242. Huchtmeier et al. (2000) observed it in the 21 cm H I line with the 100 m Effelsberg telescope and detected its H I-flux, 2.03 Jy, km s^{-1} at the radial velocity of $V_h = 426$ km s^{-1} with the H I line width of $W_{50} = 100$ km s^{-1}. The obtained radial velocity exceeds the radial velocity of NGC 6503, $V_h = +25$ km s^{-1} (Epinat et al. 2008; Greisen et al. 2009), over ∼400 km s^{-1}, and the high H I-flux and the wide H I line width do not harmonize with the low luminosity of KK 242 at its apparent magnitude $B = 18\overset{\rm m}{.}6$. Later, Koda et al. (2015) performed a deep survey of the vicinity of NGC 6503 on the Subaru telescope with Suprime-Camera and rediscovered the KK 242 dwarf system, giving it the name NGC 6503-d1. On the deep images in B, V, R, I-bands the dwarf galaxy KK 242 = NGC 6503-d1 = PGC 4689184 was resolved into stars. Based on the color–magnitude diagram (CMD) for them,

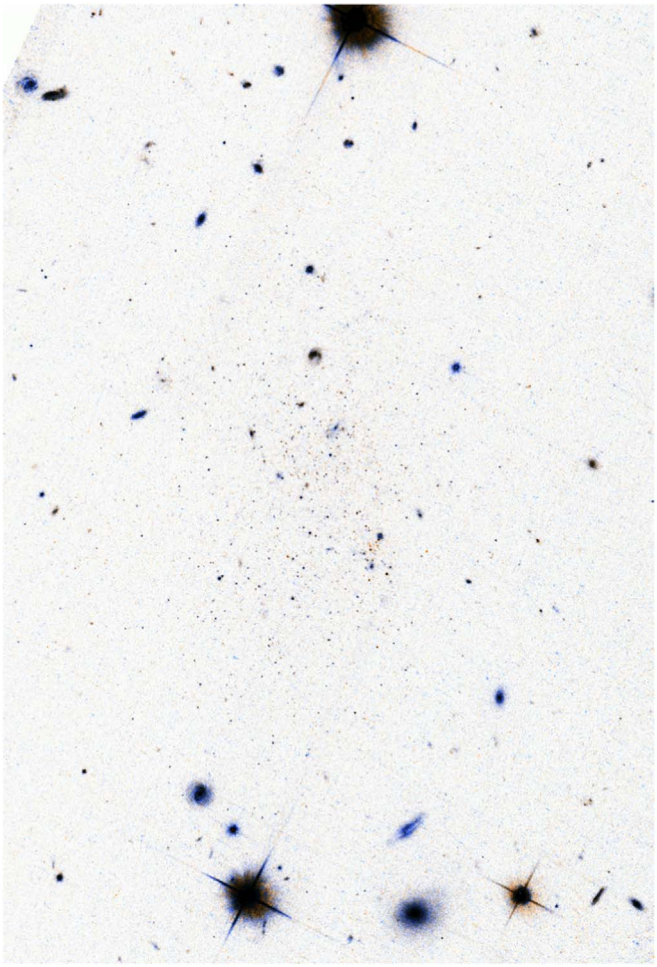

Figure 1. HST/ACS combined image of KK 242. The image size is $104'' \times 70''$. North is up and east is left. The inverted color image is composite of images with F606W and F814W filters. Blue stars are seen as red dots.

the authors estimated the dwarf galaxy distance to be at a distance of ∼5.3 Mpc. With an error in estimating the distance of ∼1 Mpc, this value is consistent with the distance of the galaxy NGC 6503 itself, $D = 6.25$ Mpc (Extragalactic Distance Database = EDD, http://edd.ifa.hawaii.edu), measured from *V*, *I* images on the Hubble Space Telescope (HST). However, to confirm the physical connection between KK 242 and NGC 6503, a more accurate measurement of the distance to KK 242 is necessary, as well as verification and refinement of its radial velocity. The measurement of these parameters is the subject of our work.

2. The TRGB Distance Derived with HST

The first observations of KK 242 with the HST were made on 1999 October 4 under the SNAP program 8192 (PI P. Seitzer). Two images of the galaxy were obtained in F606W (600 s) and F814W (600 s) filters with WFPC2 camera. The galaxy was resolved into stars, but their CMD turned out to be too shallow to determine the galaxy distance.

New observations of KK 242 were performed with the Advanced Camera for Surveys (ACS) aboard the HST on 2019 October 15 as part of the "Every Known Nearby Galaxy" survey (SNAP-15922, PI R.B. Tully). Two exposures were made in a single orbit with the filters F606W (760 s) and F814W (760 s). An inverted color cutout of the galaxy

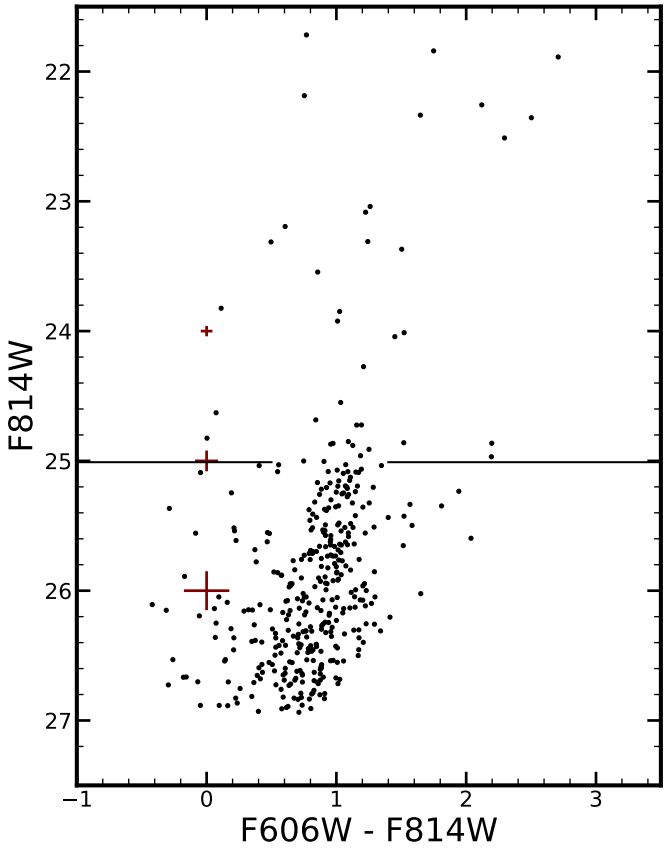

Figure 2. Color–magnitude diagram of KK 242. The TRGB position is indicated by the horizontal black line. Representative error bars (calculated at the observed color of the TRGB) are shown in maroon.

produced with this data is shown in Figure 1, with a size of $104''$ by $70''$. The galaxy contains young and older stellar population visible as red and blue dots, respectively.

We used the ACS module of the DOLPHOT package[5] by Dolphin (2000, 2016) to perform photometry of the resolved stars based on the recommended recipe and parameters. Only stars with good-quality photometry (defined as type $\leqslant 2$) were included in the analysis. We also selected stars with a signal-to-noise ratio of at least five in both filters, and with DOLPHOT parameters $(\mathrm{Crowd_{F606W}} + \mathrm{Crowd_{F814W}}) \leqslant 0.8)$, $(\mathrm{Sharp_{F606W}}+\mathrm{Sharp_{F814W}})^2 \leqslant 0.075$ (McQuinn et al. 2017). As the galaxy does not take up the entire $202''$ by $202''$ ACS field of view, we isolated the galaxy to produce a CMD which is limited in contamination from objects such as foreground stars or unresolved background galaxies.

Artificial stars were inserted and recovered using the same DOLPHOT parameters to accurately estimate the photometric errors. The resulting CMD in F606W – F814W versus F814W is plotted in Figure 2, shown along with representative error bars from the results of the artificial star experiments. We measured the magnitude of the tip of the red giant branch (TRGB) by following the methods outlined by Makarov et al. (2006) and Wu et al. (2014). We modeled the luminosity function of asymptotic giant branch and red giant branch stars as a broken power law, with the break defining the magnitude of the TRGB. The physical reason for this parameterization is that the abrupt and standard-candle nature of the onset of the helium flash presents itself as a discontinuity on the observed luminosity function. The benefit of

[5] http://purcell.as.arizona.edu/dolphot

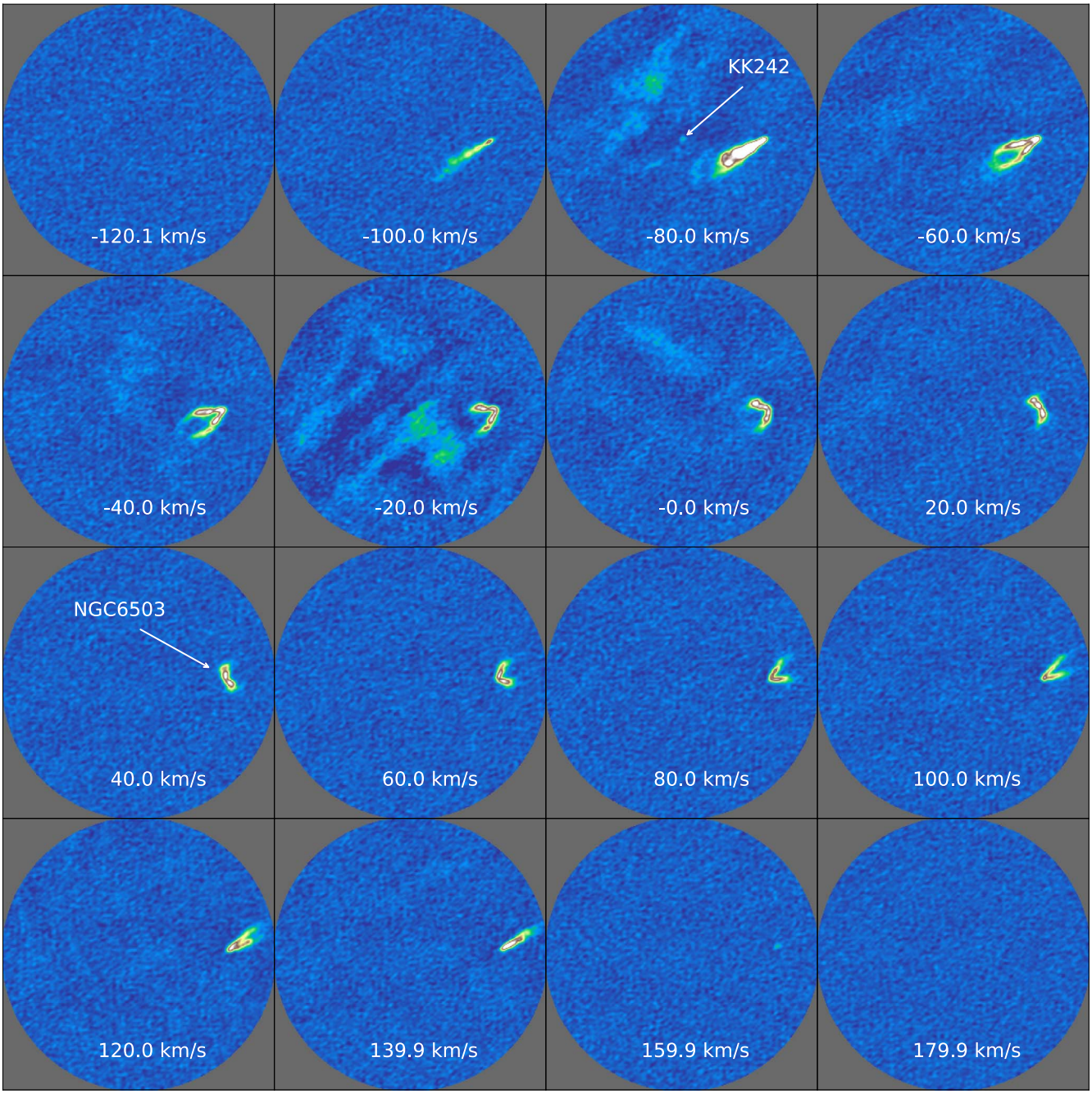

Figure 3. Channel maps showing H I emission from KK 242, the Milky Way, and NGC 6503. The velocity resolution is 20 km s^{-1} ch^{-1}, and the intensity scale spans the range from 50% of the (negative) minimum value in the cube to 50% of the (positive) maximum value in the cube. Valid pixels are shown within the VLA primary beam to the level of 5% of the maximum. Strong H I emission is detected from the field spiral NGC 6503; weaker but more widespread H I emission from the Milky Way is prominent. The tentative detection of H I gas from KK 242 is apparent in the −80 km s^{-1} panel; the compact H I source at the field center is cospatial with the optical body and co-spectral (within errors) with the emission line velocity derived by S. A. Pustilnik et al. (2021, in preparation). The field of view is 53′.3 on a side.

this procedure over a simple edge-detection algorithm (e.g., a Sobel filter) is the ability to directly incorporate the results of artificial star experiments. This is important as DOLPHOT has been shown to systematically underestimate the reported photometric errors (e.g., Williams et al. 2014). The results from the artificial star experiments are explicitly taken into account by convolving the predefined luminosity function with functions that account for completeness, photometric error, and bias. Using this procedure, we found F814W(TRGB) to be $25^{\rm m}.01 \pm 0^{\rm m}.11$. Following the zero-point calibration of the absolute magnitude of the TRGB developed by Rizzi et al. (2007), we obtained $M(\mathrm{TRGB}) = -4.11$ at W606F − W814F = 1.00. Assuming $E(B-V) = 0.032$ from Schlafly & Finkbeiner (2011) for foreground reddening, we derived a distance modulus of $(m-M)_0 = 29.05 \pm 0.11$, or the distance $D = 6.46 \pm 0.32$ Mpc. These values are somewhat larger than those obtained by Koda et al. (2015): $(m-M) = 28.61 \pm 0.23$ and $D = 5.27 \pm 0.53$ Mpc from the photometry of the brightest stars resolved with the Subaru Prime Focus Camera. The DOLPHOT photometry, full-field CMD, and a list of underlying parameters are available on the Extragalactic Distance Database's CMDs/TRGB Catalog (Anand et al. 2021).

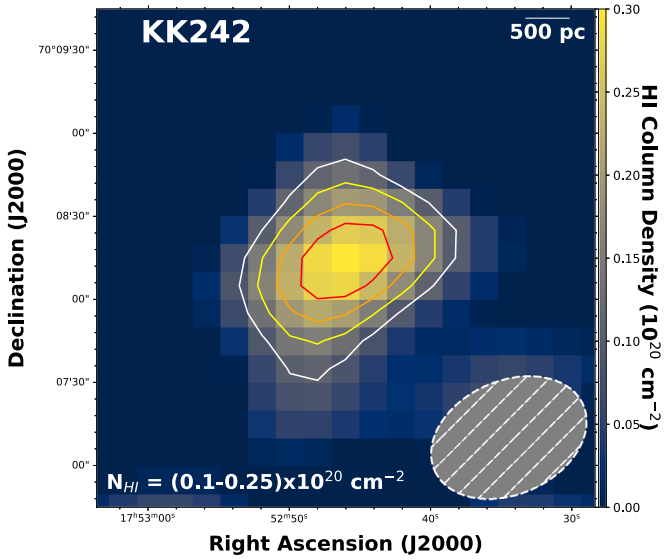

Figure 4. Integrated H I image of KK 242, created by imaging the H I in the velocity range −90 to −70 km s^{-1} and enforcing a 3.5σ threshold. The putative H I emission is very faint and of low S/N. Contours are shown in column density units at levels of (0.1, 0.2, 0.3) × 10^{20} cm^{-2}. The synthesized beam size of 58.″5 × 40.″8 is shown by the shaded ellipse at the lower right.

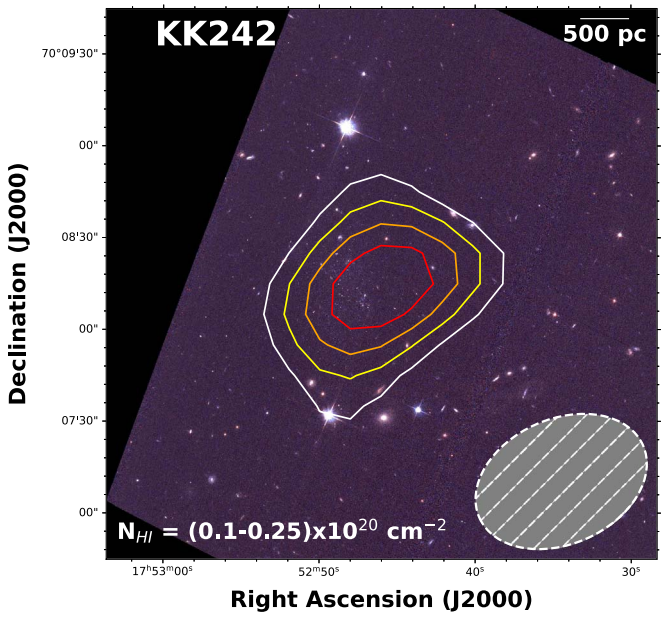

Figure 5. H I column density contours (from Figure 4) overlaid on an HST three-color image of KK 242. The H I centroid is cospatial with the optical counterpart within one half of the H I beam. The synthesized beam size of 58.″5 × 40.″8 is shown by the shaded ellipse at the lower right.

3. Ground-based Observations

3.1. Optical Observations

The galaxy KK 242 was observed on the 6 m telescope of the Special Astrophysical Observatory (SAO) with the Hα filter ($\lambda_{\rm eff}$ = 6555 Å, $\Delta\lambda$ = 74 Å) and in the midband filters SED 607 and SED 707 on 2018 April 22. The exposure time was 2 × 600 s in the Hα-line and 2 × 300 s in the continuum. After standard data processing procedures, a faint emission spot with a flux of $F(\mathrm{H}\alpha) = (4.7 \pm 2.5) \times 10^{-16}$ erg s^{-1} cm^{-2} was found on the western side of the galaxy (Kaisin & Karachentsev 2019). This value is in satisfactory agreement with the Hα-flux estimate made by Koda et al. (2015) at the Subaru telescope. The average of these two estimates corresponds to the star formation rate in KK 242 at a distance of 6.46 Mpc equal to SFR (Hα) = −4.82 dex ($M_\odot$ yr^{-1}). As noted by Koda et al. (2015), the galaxy was detected in the GALEX survey (Gil de Paz et al. 2007). With an apparent FUV-magnitude of (21.42 ± 0.15) mag, its integral star formation rate is SFR(FUV) = −4.06 dex ($M_\odot$ yr^{-1}). The brightest part of the image of KK 242 in the FUV-band coincides with the H II-region visible in the Hα line.

Recently, S. A. Pustilnik et al. (2021, in preparation) performed spectral observations of this H II-region with the SAO 6 m telescope and estimated the galaxy's heliocentric radial velocity to be $V_h = -(65 \pm 25)$ km s^{-1}. This optical velocity differs significantly from the old velocity estimate of +426 km s^{-1} obtained by Huchtmeier et al. (2000) via the H I line.

3.2. The H I-observations with VLA

KK 242 was observed with the Karl G. Jansky Very Large Array[6] (hereafter VLA) in 2019 November for program 19B-002 (P.I. Cannon). Five hours of observing time were acquired in three separate scheduling blocks. The WIDAR correlator was configured with a 16 MHz bandwidth centered on the expected recessional velocity of KK 242 (+426 km s^{-1}; Huchtmeier et al. 2000). 4096 spectral channels deliver a native spectral resolution of 3.906 kHz ch^{-1} (0.82 km s^{-1} cm^{-1} at the rest frequency of the 21 cm line of neutral hydrogen). The wide bandwidth assures ample line-free channels for accurate continuum subtraction.

Data reduction followed standard H I procedures. Briefly, radio frequency interference and bad data were excised. The absolute flux scale and bandpass shapes were determined by observations of the standard calibrator 3C 286. Gain phases and amplitudes were determined by observations of quasar J1748 +7005. The spiral galaxy NGC 6503 is within the VLA primary beam at 21 cm when observing J1748+7005. The channels containing H I line emission from this source (and the Milky Way) were blanked during the scans of the phase calibrator field. After calibration, continuum subtraction was performed in the *uv* plane using a first-order fit to line-free channels.

Imaging of the field was performed using the CASA TCLEAN algorithm (see McMullin et al. 2007). Calibrated and continuum-subtracted *uv* visibilities from all three data sets were imaged simultaneously using the AUTO-MULTITHRESH algorithm (Kepley et al. 2020). Initial H I data cubes were centered at the expected H I velocity of KK 242 (+426 km s^{-1}; Huchtmeier et al. 2000). Surprisingly, no H I emission was detected within 200 km s^{-1} at this location. The final H I cube had a synthesized beam size of ∼60″ × ∼40″ (asymmetric due to the northerly decl. of the source), a velocity resolution of 5 km s^{-1} ch^{-1}, and reached an rms noise of 9 × 10^{-4} Jy bm (within 7% of the theoretical noise level). The initial conclusion was that the source was not detected in the H I spectral line.

The recent downward revision of the recessional velocity of KK 242 by S. A. Pustilnik et al. (2021, in preparation) prompted us to reexamine the H I data products with this prior.

[6] The National Radio Astronomy Observatory is a facility of the National Science Foundation operated under cooperative agreement by Associated Universities, Inc.

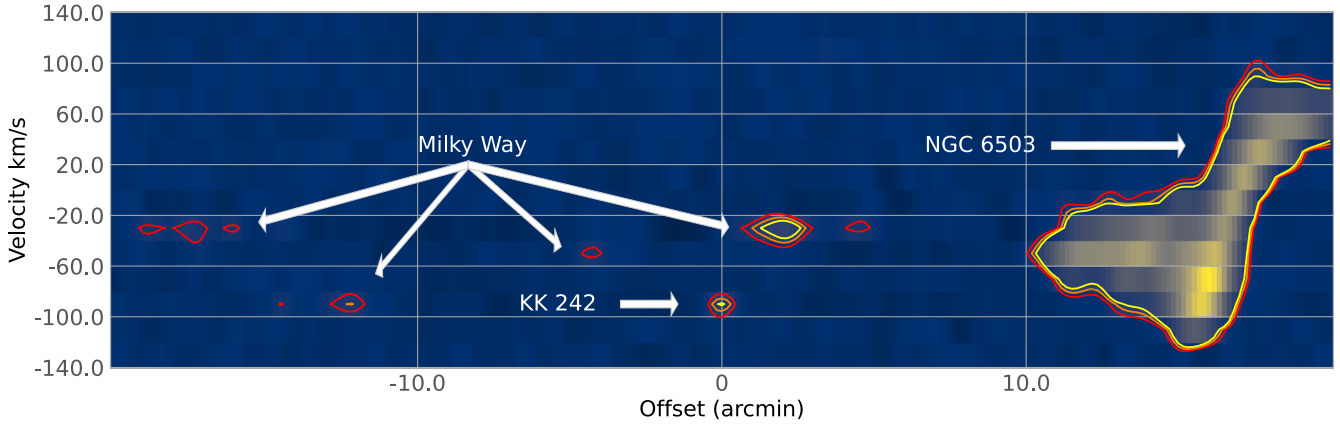

Figure 6. PV slice through the H I datacube shown in Figure 3. The 50″ wide slice is oriented east–west, passes through the H I centroid of KK 242 (see Figure 4), and extends ±20′. The slice intersects the putative H I gas associated with KK 242 as well as with the disk of NGC 6503 and with multiple foreground Milky Way H I clouds. Contours are shown at levels of 4, 5.5, and 7σ. This *P*–*V* diagram suggests that the faint H I emission that is cospatial with the optical body of KK 242 is distinct in both position and velocity space from other H I structures in the field.

Table 1
Properties of KK 242

R.A. (J2000)	17 52 48.4
Decl. (J2000)	+70 08 14
Type	Transition
D, Mpc	6.46 ± 0.32
$V_{\rm hel}$, km s^{-1}	−80 ± 10
B, mag	18.6
M_B, mag	−10.5
SFR(Hα), $M_\odot$ yr^{-1}	−4.82 dex
SFR(FUV), $M_\odot$ yr^{-1}	−4.06 dex
log(M_*), $M_\odot$	6.47
S(H I), Jy km s^{-1}	<0.1
log($M_{\rm H\,I}$), $M_\odot$	<6.0

As Figure 3 shows, the H I gas from NGC 6503 and from the Milky Way are both prominent in the velocity range between −100 and 0 km s^{-1}. These two contaminants have high surface brightnesses over a range of angular scales, resulting in a very complicated distribution of flux in the cubes. Identifying the H I-flux from KK 242 is nontrivial.

After examining H I data cubes with a range of velocity resolutions, we identified weak emission that is spatially coincident with the optical position of KK 242 in the velocity range −90 to −70 km s^{-1}. To maximize the signal-to-noise ratio (S/N) of the H I gas from KK 242, we created a datacube with 20 km s^{-1} velocity resolution. The channel spacing was selected empirically to place all of the apparent H I emission from KK 242 into a single channel of the resulting datacube. The AUTO-MULTITHRESH algorithm was used to identify signal in the field (which can arise from the Milky Way, from NGC 6503, or from KK 242), which surpasses the 3.5σ level in each channel. Inside of these regions the cube was cleaned to a level of 0.5σ (where $\sigma = 4.5 \times 10^{-4}$ Jy bm^{-1} in 20 km s^{-1} channels that are completely free of H I emission).

We detect very faint H I emission that is spatially and spectrally coincident with KK 242. The source is visible in the center of the $V = -80$ km s^{-1} panel of the channel maps shown in Figure 3. Since the gridding of the H I data was chosen to encompass all of the apparent H I emission from the source, this individual channel map can be immediately converted into a moment zero image (representing total H I mass surface density) by multiplying by the channel width. Figure 4 shows this representation of the H I data, calibrated in units of H I column density. The peak column density is a very modest $\sim 3 \times 10^{19}$ cm^{-2}. The source is effectively unresolved by the (asymmetric) beam. Figure 5 shows the same H I column density contours overlaid on a color image of KK 242 using data from the Legacy Survey. There is positional agreement of the H I and optical components within half of the H I beam diameter.

The complicated nature of the H I in the spatial and spectral regions surrounding KK 242 demands scrutiny about the reality of the source and the significance of the detection. To further examine the H I properties, Figure 6 shows a position–velocity (PV) slice through the H I datacube. The ±40′ long PV slice was taken at an angle of +270° (measured eastward from north), was centered on the H I maximum of KK 242 (determined from the moment zero map; see Figure 4), and was integrated over a width of 5 pixels (corresponding roughly to the H I beam diameter). The resulting PV slice shown in Figure 6 emphasizes that the H I gas that is associated with KK 242 is offset both spectrally and spatially from the H I emission from the Milky Way and NGC 6503.

While Figures 3–6 are suggestive of the H I being associated with the low-mass galaxy KK 242, the emission is of very low S/N and should be interpreted with caution. Indeed, without the velocity prior from S. A. Pustilnik et al. (2021, in preparation), the putative source would not have been identified. Below we put forth some simplistic interpretations of the H I properties on the assumption that the H I gas is in fact associated with KK 242. We stress that these interpretations should be considered as demonstrative only. More sensitive observations are required to verify the putative detection. The Huchtmeier et al. (2000) detection at +426 km s^{-1} remains a puzzle for us. If there was an H I signal of that strength (2.03 Jy, km s^{-1}) in the velocity range of the VLA then we would have detected it easily.

Integrating the H I emission in the single-channel moment map, we find a total H I-flux integral $S_{\rm H\,I} < 0.1$ Jy km s^{-1} with an error of no less than 50%. At the distance of 6.46 Mpc, the corresponding H I mass is less than 10^6 $M_\odot$. This H I mass is comparable to that of the famous Local Volume galaxy Leo P (McQuinn et al. 2015 and references therein) and lower than all of the H I masses in the SHIELD program (McNichols et al. 2016; Teich et al. 2016). The S/N of the H I data is too low to derive a velocity field for KK 242, and so its rotational velocity

Table 2
Detached Spiral Sc–Sd Type Galaxies in the Local Volume with $\log(L_K/L_\odot) = 9.5$–10.0, and their Probable Companions

Name	T	D (Mpc)	meth	V_{LG} (km s^{-1})	$\log L_K$ ($L_\odot$)	V_{rot} (km s^{-1})	R_p (kpc)	ΔV (km s^{-1})	M_T ($10^{10} M_\odot$)
(1)	(2)	(3)	(4)	(5)	(6)	(7)	(8)	(9)	(10)
M33	6	0.93	trgb	34	9.62	99	0	0	
And XXII	−3	0.79	trgb	87	5.28		47	53	15.6
Tri III	−3	0.82	trgb	⋯	4.43		82	⋯	⋯
NGC 2403	6	3.19	trgb	262	9.86	128	0	0	
MADCASHJ0742+65	−2	3.39	trgb	⋯	5.86		36	⋯	⋯
DDO 44	−3	3.21	trgb	356	7.78		73	94	76.1
NGC 2366	9	3.28	trgb	251	8.70		206	−11	2.9
NGC 7793	6	3.63	trgb	250	9.70	101	0	0	
PGC 704814	10	3.66	trgb	299	6.90		14	49	4.0
NGC 1313	7	4.31	trgb	264	9.57	120	0	0	
[KK 98]27	10	4.23	trgb	327	7.04		25	63	11.7
NGC 4236	8	4.41	trgb	157	9.61	70	0	0	
[KK 98]125	10	4.40	mem	⋯	6.61		50	⋯	⋯
DDO 165	9	4.83	trgb	196	8.23		374	39	67.1
NGC 5068	6	5.15	trgb	469	9.73	66	0	0	
dw1318-21	−1	5.15	mem	⋯	7.06		78	⋯	⋯
NGC 6503	6	6.25	trgb	283	10.00	91	0	0	
[KK 98]242	10	6.46	trgb	178	6.47		31	−105	40.3
NGC 4656	8	7.98	trgb	635	9.93	64	0	0	
NGC 4656UV	10	7.98	mem	568	8.88		40	−67	21.2
NGC 7640	6	8.43	trgb	668	9.77	107	0	0	
UGC 12588	8	8.43	mem	723	8.83		103	55	36.8
DDO 217	8	8.55	TF	720	9.37		219	52	69.9
Average	⋯	⋯	⋯	⋯	⋯	94 ± 8	98 ± 27	$+22 \pm 21$	34.6 ± 8.4

and total mass remain unconstrained by the H I data as presented here.

4. Halo Mass of NGC 6503 and Other Nearby Low-mass Spirals

Table 1 gives some basic properties of KK 242, including its equatorial coordinates, morphological type, distance, heliocentric radial velocity, apparent and absolute B magnitudes, star formation rates estimated via Hα and FUV-fluxes, stellar mass, (putative) H I-flux, and the total hydrogen mass. Other photometric parameters of the galaxy (its color, surface brightness, and effective radius) can be found in Koda et al. (2015).

Assuming the Keplerian motions of small satellites around a central massive galaxy with a typical eccentricity $e = 0.7$, we can estimate the total mass of the main galaxy from the radial velocity difference, ΔV, and projected separation, R_p, of its satellite (Karachentsev & Kudrya 2014):

$$M_T = (16/\pi) G^{-1} \Delta V^2 R_p,$$

where G is the gravitation constant. This expression is based on the assumption that the orbits of satellites are oriented randomly relative to the line of sight. For the pair of NGC 6503 and KK 242 at $\Delta V = 105$ km s^{-1} and $R_p = 31$ kpc, this mass estimate is $4.03 \times 10^{11} M_\odot$. Obviously, this estimate is subject to significant uncertainty due to the projection factor affecting ΔV and R_p. To get a more robust idea of the total mass of spiral galaxies of moderate luminosity, we selected from the Updated Nearby Galaxy Catalog (UNGC; Karachentsev et al. 2013) isolated Sc–Sd galaxies with luminosities in the K-band $L_K/L_\odot = (9.5$–$10.0)$ dex, in which small satellites have been found. In total, there are nine such galaxies in the Local Volume with a radius of 10 Mpc, around which 14 satellites are found, and 10 of them have measured radial velocities. For all nine spiral galaxies, the distances were measured with an accuracy of ∼5% by the TRGB method. Data on these galaxies and their companions are presented in Table 2. The Table columns contain: (1) galaxy name; (2) morphological type according to de Vaucouleurs scale; (3) galaxy distance; (4) method used to determine the distance (via the tip of TRGB, from the Tully–Fisher relation (TF), based on a probable membership of the dwarf galaxy in the suite of main galaxy (mem)); (5) radial velocity of galaxy relative to the Local Group centroid; (6) logarithm of integral luminosity of galaxy in the K band; (7) maximum amplitude of galaxy rotation; (8), (9) projected separation and radial velocity difference of companion relative to the main galaxy; (10) estimate of the total (orbital) mass. The data on the galaxies are taken from the last version of the UNGC (http://www.sao.ru/lv/lvgdb) supplemented with recent distance estimates from EDD. Several conclusions can be drawn from the analysis of this data.

1. The root mean square radial velocity of satellites relative to the main galaxy is $\sigma_v = (63 \pm 7)$ km s^{-1}. Taking into account the average projection factor, $\sqrt{3}$, the characteristic spatial velocity of satellites, (108 ± 12) km s^{-1}, is similar to the average rotation amplitude of the spiral galaxies, (94 ± 8) km s^{-1}.

2. The mean total (orbital) mass of the spiral galaxies of moderate luminosity is $\langle M_T/M_\odot \rangle = (3.46 \pm 0.84) \times 10^{11}$. The characteristic virial radius of the halo $R_{\rm vir} \simeq 150$ kpc corresponds to this mass. The average projected separation of the satellites presented in Table 2, $\langle R_p \rangle = (98 \pm 27)$ kpc, when multiplied by the projection factor $(4/\pi)$, is in good agreement with $R_{\rm vir}$.
3. The mean luminosity of the considered spiral galaxies, $\langle L_K/L_\odot \rangle = (6.0 \pm 1.4) \times 10^9$, is about an order of magnitude lower than the luminosity of Milky Way and M31. The ratio of the average halo mass-to-average K luminosity for them is $(58 \pm 19) M_\odot/L_\odot$, which is slightly higher than the M_T/L_K for Milky Way, $(27 \pm 9) M_\odot/L_\odot$ and M31, $(33 \pm 6) M_\odot/L_\odot$ (Karachentsev & Kudrya 2014), also obtained from the motion of their satellites.

5. Concluding Remark

The isolated spiral galaxy NGC 6503 (a.k.a. KIG 837 in the Catalog of Isolated Galaxies; Karachentseva 1973), and its faint companion KK 242 are on the border of the Local Void (Tully 1988). According to Tully et al. (2008), the center of the Local Void is at a distance of ∼(10–20) Mpc from us, and the galaxies on the Void border are moving from its center at a velocity of ~ 280 km s^{-1}. Located between the center of the expanding Void and the observer, the NGC 6503 and KK 242 pair should have a negative peculiar velocity for us. Indeed, at the measured distances and line-of-sight velocities and adopting the Hubble parameter $H_0 = 73$ km s^{-1} Mpc^{-1}, the peculiar velocities of both galaxies, $V_{\rm pec} = V_{\rm LG} - H_0 D$, are -173 km s^{-1} and -294 km s^{-1}, respectively, confirming the concept of the Local Void expansion.

Away from NGC 6503, opposite the Local Void, there is a chain of groups around massive spiral galaxies: M101, M51, and M63, the distances D and radial velocities $V_{\rm LG}$ of which smoothly increase with separation from NGC 6503 and the Local Void boundary: 6.95 Mpc and $+375$ km s^{-1} (M101), 8.40 Mpc and $+553$ km s^{-1} (M51) and 9.04 Mpc and 570 km s^{-1} (M63). This circumstance was noted by Müller et al. (2017). Interestingly, the distance (6.25 Mpc) and radial velocity ($+283$ km s^{-1}) of the NGC 6503 fits well the configuration of this chain. Together with NGC 6503, the angular extent of this filament in the sky reaches about 30°.

This work is based on observations made with the NASA/ESA Hubble Space Telescope and with the Very Large Array.

J.M.C., J.F., and J.L.I. are supported by NSF/AST-2009894.

Support for program SNAP-15922 (PI Tully) was provided by NASA through a grant from the Space Telescope Science Institute, which is operated by the Associations of Universities for Research in Astronomy, Incorporated, under NASA contract NASb5-26555. I.D.K. is supported in part by RNF grant 19–12–00145.

ORCID iDs

John M. Cannon https://orcid.org/0000-0002-1821-7019
R. Brent Tully https://orcid.org/0000-0002-9291-1981
Gagandeep S. Anand https://orcid.org/0000-0002-5259-2314

References

Anand, G. S., Rizzi, L., Tully, R. B., et al. 2021, AJ, 162, 80
Bilicki, M., Dvornik, A., Hoekstra, H., et al. 2021, A&A, 653, A82
Carlin, J. L., Sand, D. J., Price, P., et al. 2016, ApJ, 828L, 5
Carlsten, S. G., Greco, J. P., Beaton, R. L., & Greene, J. E. 2020, ApJ, 891, 144
Correa, C. A., & Schaye, J. 2020, MNRAS, 499, 3578
Dolphin, A. E. 2000, PASP, 112, 1383
Dolphin, A. E. 2016, DOLPHOT: Stellar Photometry, Astrophysics Source Code Library, ascl:1608.013
Epinat, B., Amram, P., Marcelin, M., et al. 2008, MNRAS, 388, 500
Gil de Paz, A., Boissier, S., Madore, B. F., et al. 2007, ApJS, 173, 185
Greisen, E. W., Spekkens, K., & van Moorsel, G. A. 2009, AJ, 137, 4718
Huchtmeier, W. K., Karachentsev, I. D., Karachentseva, V. E., & Ehle, M. 2000, A&AS, 141, 469
Kaisin, S. S., & Karachentsev, I. D. 2019, AstBu, 74, 1
Karachentsev, I. D., & Kudrya, Y. N. 2014, AJ, 148, 50
Karachentsev, I. D., Makarov, D. I., & Kaisina, E. I. 2013, AJ, 145, 101
Karachentseva, V. E. 1973, Soobschenia Spec. Astrophys. Obs., 8, 3
Karachentseva, V. E., & Karachentsev, I. D. 1998, A&AS, 127, 409
Karachentseva, V. E., Karachentsev, I. D., & Melnyk, O. V. 2011, AB, 66, 389
Kepley, A. A., Tsutsumi, T., Brogan, C. L., et al. 2020, PASP, 132, 024505
Koda, J., Yagi, M., Komiyama, Y., et al. 2015, ApJL, 801, L24
Kourkchi, E., & Tully, R. B. 2017, ApJ, 843, 16
Lapi, A., Salucci, P., & Danese, L. 2018, ApJ, 859, 2
Makarov, D. I., Makarova, L. N., Rizzi, L., et al. 2006, AJ, 132, 2729
Martin, N. F., McConnachie, A. W., Irwin, M., et al. 2009, ApJ, 705, 758
Martinez Delgado, D., Karim, N., Boschin, W., et al. 2022, MNRAS, 509, 16
McMullin, J. P., Waters, B., Schiebel, D., Young, W., & Golap, K. 2007, in ASP Conf. Ser. 376, Astronomical Data Analysis Software and System, ed. R. A. Shaw, F. Hill, & D. J. Bell (San Francisco, CA: ASP), 127
McNichols, A. T., Teich, Y. G., Nims, E., et al. 2016, ApJ, 832, 89
McQuinn, K. B. W., Skillman, E. D., Dolphin, A., et al. 2015, ApJ, 812, 158
McQuinn, K. B. W., Skillman, E. D., Dolphin, A., et al. 2017, ApJ, 154, 51
Müller, O., Scalera, R., Binggeli, B., & Jerjen, H. 2017, A&A, 602A, 119
Posti, L., & Fall, S. M. 2021, A&A, 649, A119
Rizzi, L., Tully, R. B., Makarov, D. I., et al. 2007, ApJ, 661, 815
Schlafly, E. F., & Finkbeiner, D. P. 2011, ApJ, 737, 103
Teich, Y. G., McNichols, A. T., Nims, E., et al. 2016, ApJ, 832, 85
Tollerud, E. J., Beaton, R. L., Geha, M. C., et al. 2012, ApJ, 752, 45
Tully, R. B. 1988, Nearby Galaxy Catalog (Cambridge: Cambridge Univ. Press)
Tully, R. B., Shaya, E. L., Karachentsev, I. D., et al. 2008, ApJ, 676, 184
Williams, B. F., Lang, D., Dalcanton, J. J., et al. 2014, ApJS, 215, 9
Wu, P. F., Tully, R. B., Rizzi, L., et al. 2014, AJ, 148, 7